Journal of The Electrochemical Society, **162** (12) E277-E281 (2015)
0013-4651/2015/162(12)/E277/5/$33.00 © The Electrochemical Society

Effective Reduction of Copper Surface for Clean Graphene Growth

Hak Ki Yu[z]

Department of Energy Systems Research, Ajou University, Suwon 443-739, Korea
Department of Materials Science and Engineering, Ajou University, Suwon 443-739, Korea

We developed a new pre-reduction method of Cu surface (using $(NH_4)_2S_2O_8$ etching solution) for high quality graphene growth. The adsorbed oxygen and water molecules on the bare Cu surface produce CuO_2 and $Cu(OH)_2$ bonding, resulting in physical degradation of continuous monolayer graphene by forming CuO_x nano-particles at the interface between graphene and Cu catalyst. The chemical degradation of graphene was also confirmed by analyzing the sp^3 / sp^2 C-C bond ratio using X-ray photoemission. The conventional reduction method such as hydrogen reduction and acetic acid pre-treatment was not sufficient to remove these CuO_x nano-particles. We demonstrated that the pre-etched Cu foil in 0.3 mole $(NH_4)_2S_2O_8$ solution for 1 min can be the most ideal candidate for the high quality and clean graphene growth.

Manuscript submitted July 21, 2015; revised manuscript received August 21, 2015. Published September 2, 2015.

Due to its ease of implementation, the use of Cu foils to catalyze graphene formation by chemical vapor deposition (CVD) in a methane-hydrogen atmosphere has been widely implemented.[1,2] This may even be fair to say that it is the most commonly used method for the bottom up production of graphene. It has numerous advantages in addition to its simplicity. These include: minimal formation of multilayers, large total graphene sample size, large grain size in the 2D poly-crystal, and the ability to transfer the graphene to another substrate.[3–5]

In efforts to produce large, flat, single layer graphene samples with large domain sizes, we carried out a careful and comprehensive analysis of the steps needed to transform methane and hydrogen to high quality graphene using the Cu foil catalyzed CVD. An important finding of this work is the influence of the oxidation state of the Cu catalyst, which is a crucially important aspect of the synthesis.[6–8] Improper attention to the reduction of the Cu catalyst can lead to numerous problems. The sp^3 / sp^2 C-C bonds ratio of the graphene sample can be increased due to the C-O bond formation in the graphene layer. The grain size of the graphene can be reduced. It is also possible to form CuO_x particles on the catalyst. These particles influence the rate of growth of the graphene and even when growth is rapid, they enhance the "wrinkling" of the graphene product. This "wrinkled graphene" is more subject to damage and the formation of filaments upon transfer to another substrate. Due to the formation of Cu-O-C bonding moieties, the Cu may be transferred with the graphene sample, with unknown consequences for the properties of the material.[9] In contrast, when careful attention is paid to the complete reduction of the Cu catalyst, extremely high quality graphene samples can be obtained. In this paper, we report a detailed analysis of this commonly used graphene synthesis.

The oxidation of a Cu surface (such as CuO, Cu_2O, or $Cu(OH)_2$) is easily processed at room temperature since the Gibbs free energies of formation for CuO, Cu_2O, and $Cu(OH)_2$ are −31.9, −38.13, and −85.5 kcal/mol, respectively.[10] Because these native oxides could reduce the catalytic activity for graphene growth, pre-annealing of Cu foil in a hydrogen reducing atmosphere at 1000°C is essential in conventional CVD graphene growth.[11,12] Although the hydrogen reducing annealing could help to clean the surface of the Cu foil, some of the remaining Cu oxides segregated as nanoparticles with some impurities influence the interaction of the catalytic activity for graphene growth as shown in Fig. 1a. Although a number of alternative solutions (pre-chemical treatment in acetic acid and hydrochloric acid or electro-mechanical polishing) have been studied, the ability to remove the Cu oxide nanoparticles is not ideal (see Fig. 1b) and other processes such as polishing are quite cumbersome.[13–16] Therefore, in this work, we etched the top surface of the Cu foil by dipping in $(NH_4)_2S_2O_8$ solution before CVD growth as shown in Fig. 1c. The etching solution of Cu using $(NH_4)_2S_2O_8$ is free from the contamination of ferrous ions compared to Fe^{3+} based etching solution such as $Fe(NO_3)_3$ and $FeCl_3$. Moreover, it is more controllable than other acids such as HCl and HNO_3 because the Cu is located below hydrogen in the activity series.

Experimental

Graphene growth.— To make graphene on commercial Cu foil (Alfa Aesar, item No. 13382, 99.8% purity), the Cu foils were first immersed in 0.3 mole ammonium persulfate ($(NH_4)_2S_2O_8$, Sigma-Aldrich, item No. 248614, ACS reagent, ≥ 98.0%) solution for 1 min and then loaded into the quartz tube reaction chamber. The typical growth process is as follows. (1) The pressure in the growth chamber was pumped down to 3 mTorr using a mechanical pump. (2) A 40 sccm flow of hydrogen gas was introduced into the chamber at 950 mTorr. (3) The Cu foils were then heated to 1000°C for 60 min and annealed for 30 min to enlarge the Cu grains and remove any residual Cu oxide and impurities. (4) A 6 sccm flow of methane gas with 20 sccm hydrogen was introduced into the chamber for 10 min with a total pressure of 460 mTorr for graphene synthesis. (5) After growth, the furnace was cooled down rapidly to room temperature under a 20 sccm flow of hydrogen.

Graphene transfer.— To transfer the graphene samples, one side of the graphene/Cu foils was first spin coated with polymethyl methacrylate (PMMA) on a spin coater at 2000 rpm for 60 s and dried in atmosphere for 1 hour. The uncoated side of the graphene samples (the side that is polymer free) was then etched in an oxygen plasma for 30 sec at 100 W to remove the carbon. After the Cu foils were totally etched away in $(NH_4)_2S_2O_8$ solution (0.3 M) for 12 hours, the floating graphene/PMMA films were washed in several cycles with DI water. The resulting graphene/PMMA films were transferred onto a target substrate and dried at ambient conditions for 24 hours before being heat treated at 180°C for 30 min to increase the adhesion between the graphene and target substrate (SiO_2 covered Si substrate or TEM Cu-grid). Finally, the PMMA layers were then removed sequentially by washing with acetone, isopropyl alcohol, and de-ionized water.

Characterization of samples.— X-ray photoemission spectra (XPS) were obtained at the 8A1 beam line at the Pohang Light Source (PLS). The transmission electron microscopy (TEM) images were collected using a Philips CM12 instrument with a LaB_6 filament operated at an electron energy of 80 keV. The Raman spectra were obtained with a LabRAM HR 800 (HORIBA Yvon GmbH) spectrometer under the following conditions: excitation wavelength of the laser, He-Ne 633 nm; spot size of the laser beam, 5 μm in diameter; measurement time, 20 sec. Surface investigations were performed using a scanning electron microscope (SEM) with a 10 keV accelerating voltage.

[z]E-mail: hakkiyu@ajou.ac.kr

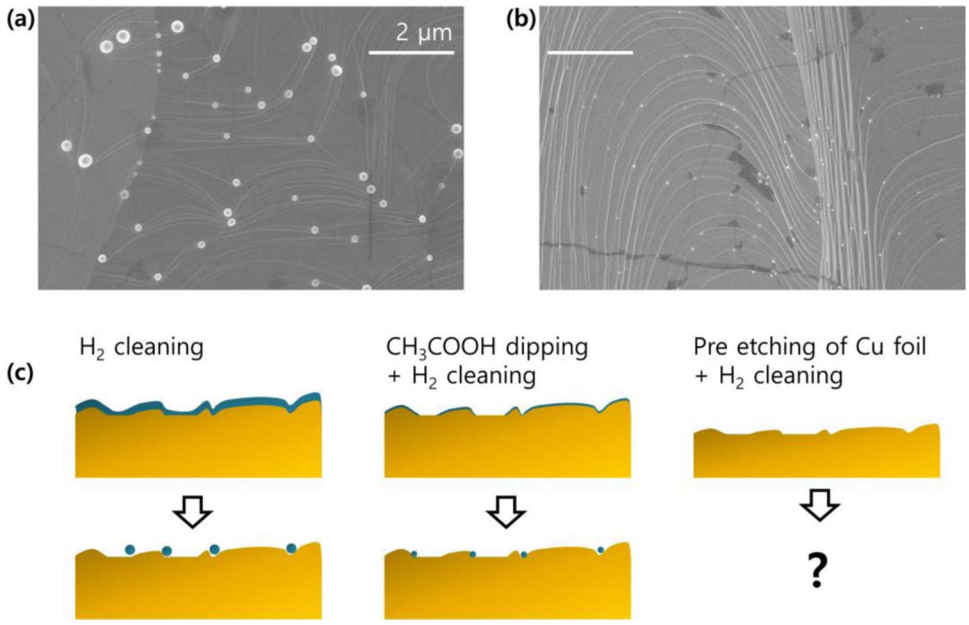

Figure 1. SEM images of graphene on Cu foil (a) only H_2 flowing during graphene growth without pre-treatment and (b) H_2 flowing and pre-treatment of Cu foil using CH_3COOH. (c) Schematic view of experimental idea (pre-etching of Cu foil before graphene growth) compared to conventional Cu reduction method. The deep yellow is Cu foil and the blue color is surface contamination layer of Cu foil such as $Cu(OH)_2$, CuO, and CuO_2.

Results and Discussion

The natural line strips of the commercial Cu foil were blurred with respect to etching time (as seen in Fig. 2b). We had measured several surface morphologies using an optical microscope after heating the Cu foils in a CVD chamber and cooling. When the heating temperature was 700°C (cooling line 1 in Fig. 2a), no significant difference was observed, although the blurred morphologies of the etched surface had slightly recovered. However, at the heating temperature of 1000°C (without methane injection, cooling line 2), the morphologies were totally recovered and the pre-etched samples were smoother than the reference samples. The final morphologies, following cooling line 3, have special characteristics as graphene was grown on the Cu surface. For the reference samples, a large number of black spots had distributed linearly as shown in the SEM images in Fig. 1a. However, these black spots had totally disappeared for the samples with pre-etching in $(NH_4)_2S_2O_8$. Compared to cooling line 2, further wrinkles were observed, which were unavoidable due to the difference in the thermal expansion coefficient between Cu and the graphene layer.

Before pre-etching in $(NH_4)_2S_2O_8$ solution, the Cu foil has several line strips and the randomly roughened surface slowly changed with respect to etching time from 1 min to 8 min (shown in Fig. 3a). Because the Cu is face centered cubic crystal, the (100) plane and its family plane has higher etching speed than the close packed (111) plane, resulting in anisotropic etching and specific tetrahedron facet surfaces for the samples etched for a long time (8 min) as shown in Fig. 3a.[17,18] As shown in Fig. 3b, for the graphene grown in a short period of time (step 3 is 1 min) at 1000°C, the density of graphene grains decreased with respect to the increase in the pre-etching time because a large number of tetrahedron facets are covered by the (100) Cu planes because the nucleation of graphene is preferred on the (111) surface compared to the (100) surfaces. The nano-size white spheres with a high concentration of oxygen compared to graphene are only seen in the sample without pre-etching. This means that pre-etching before growth is very helpful to reduce the contaminant based on Cu oxides during growth. The graphene layers with wrinkles due to the difference in the thermal expansion coefficient (graphene: -6×10^{-6}/K and Cu: 24×10^{-6}/K at room temperature) had totally covered the entire Cu foil when the growth time increased (step 3 is 10 min, Fig. 3c).[19] The samples with 1 min pre-etching show the cleaner graphene surfaces than the samples without pre-etching (the large number of Cu oxide nano-spheres changes the wrinkle patterns of graphene) and those with a long pre-etching time (many bi-layered graphene zones) samples. The origin of the large bilayer graphene area for the sample pre-etched for a long time is related to the lower nucleation density of graphene on a tetrahedron facet. Because the total dissolved carbon in the Cu matrix is the same between the pre-etched samples, the samples with many tetrahedron faces can have a relatively lower area for graphene nucleation, resulting in a partial multi-layer. This means that we can even control the number of graphene layers by controlling the pre-etching time.

Near the top of the surface, information including the composition and chemical bonding could be easily analyzed by measuring the core level X-ray photoemission (XPS) spectrums. Figure 4a shows the O *1s* core level peak of the Cu surface before the graphene growth. Due to pre-etching, we can clearly reduce the intensity of not only the $Cu(OH)_2$ peak but also the CuO_x peak. Because the measurement was performed in ex-situ, we cannot avoid the rapid oxidation of Cu after the pre-etching process. The important feature in Fig. 4a is the increase of oxygen adsorb (physical bonding with Cu surface) for the pre-etched Cu surface. The adsorbed oxygen has very weak bonding with Cu, resulting in easy reduction during the graphene growth process in the hydrogen gas environment. The C *1s* core level peak of the graphene surface could be deconvoluted into sp^2 C–C binding (284.7 eV), sp^3 C–C binding (285.2 eV), C–O single binding (285.8 eV for C-OH and 286.7 eV for C-O-C), and C=O double binding (288.3 eV for C=O and 288.9 eV for O=C-O-C).[20,21] These deconvolutions can be clearly seen for the partially covered graphene samples with many CuO_x nanoparticles (short graphene growth time, step 3 is 1 min with no-pretreatment). Compared to this sample, the other graphene samples (step 3 is 10 min) have strong sp^2 C-C bonds intensity compared to sp^3 C-C, C-O, and C=O bonds as shown in Fig. 4b. However, in detail, the presence of the Cu oxide nanoparticles (shown in the 0 min pre-etching sample) correlates to the higher intensity of the C-O bonds in the graphene sample. Therefore, high quality graphene samples with high sp^2/sp^3 ratio could be acquired by using the pre-etching method before CVD growth.

Removing the Cu oxide nanoparticles by pre-etching leads to a higher quality of transferred graphene on the SiO_2/Si substrate as shown in Fig. 5a, because the nanoparticles remaining between the

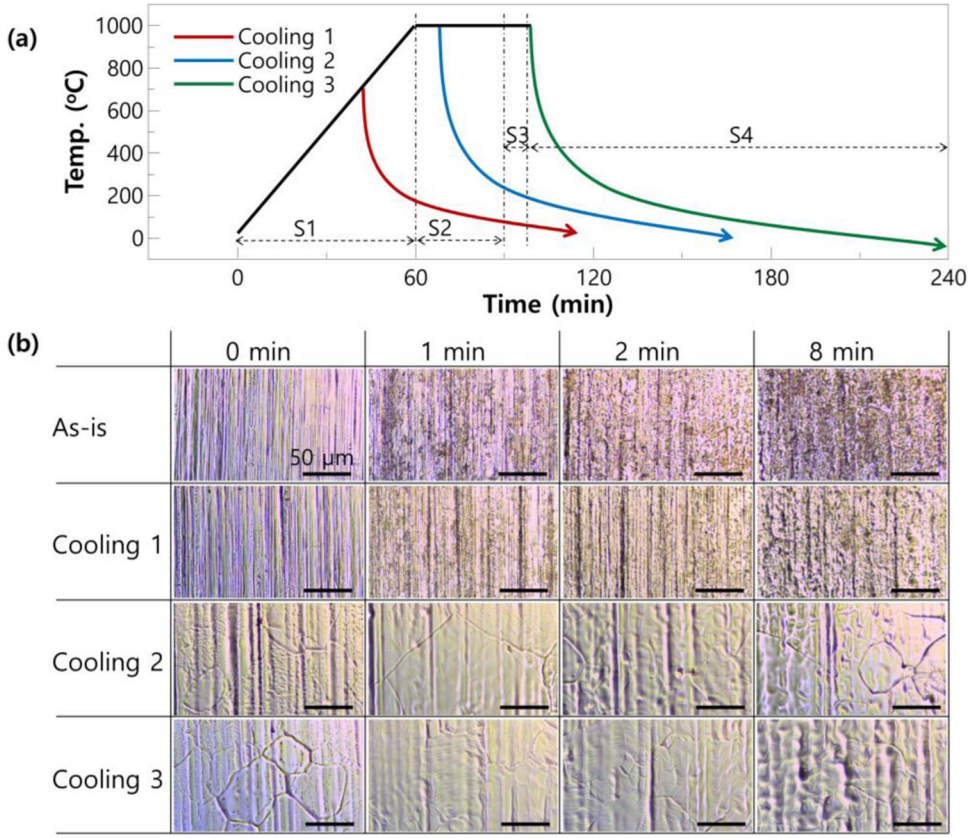

Figure 2. (a) Time-temperature curve to observe surface morphology evolution of pre-etched Cu foils with respect to graphene growth process: step 1 (S1) is the heating stage with H_2 ambient; step 2 (S2) is the annealing stage at 1000°C and H_2 ambient; step 3 (S3) is the methane insertion stage; and step 4 (S4) is the cooling stage. Cooling line 3 shows the conventional graphene growth process. We checked the additional two temperature steps; cooling line 2 refer to cooling without S3 at 1000°C and cooling line 1 means that cooling at 700°C. (b) Optical microscope images of pre-etched Cu foils (several pre-etching times: 0, 1, 2, and 8 min) based on different cooling lines shown in Fig. 2a.

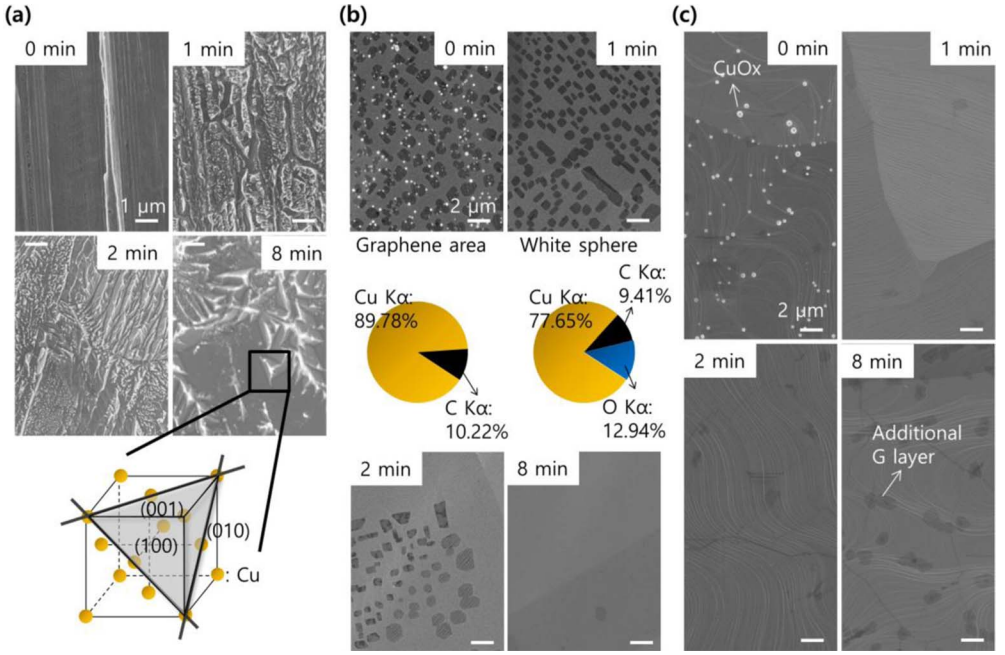

Figure 3. SEM images of pre-etched Cu surfaces (pre-etching times are 0, 1, 2, and 8 min) (a) before graphene growth, (b) after graphene growth (S3 time is 1 min), and (c) after graphene growth with the S3 time of 10 min. Elemental analysis of impurity particles and graphene (inset of Fig. 3b) obtained by area resolved energy dispersed X-ray spectroscopy (EDX).

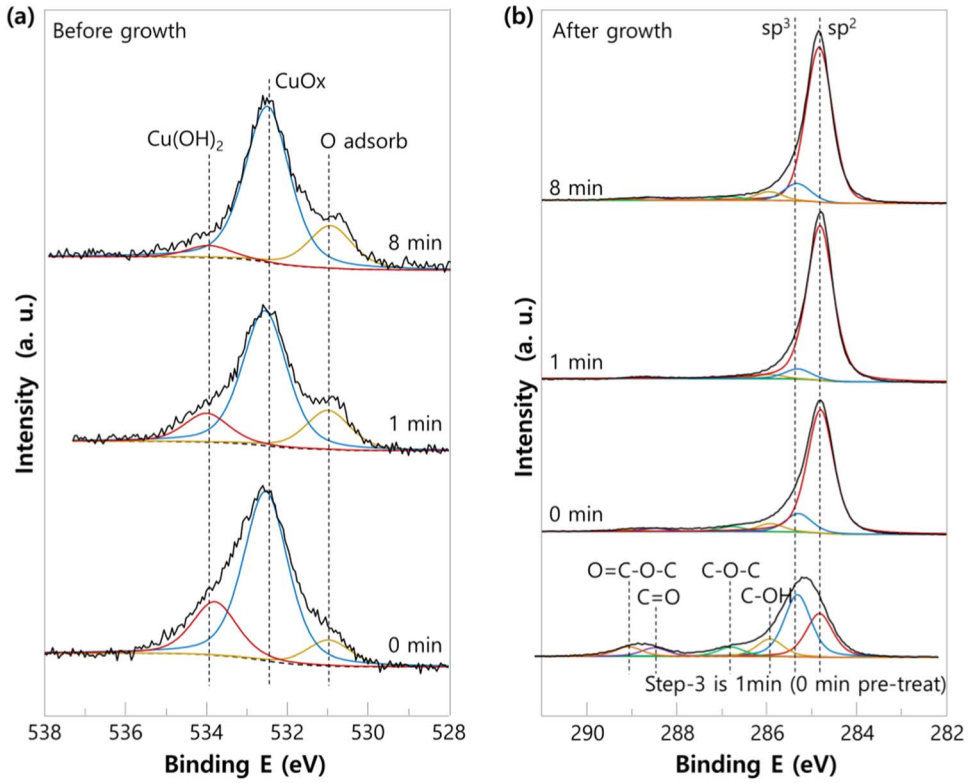

Figure 4. X-ray photoemission spectra of (a) O *1s* for the pre-etched Cu foils before graphene growth and (b) C *1s* after graphene growth with a S3 time of 10 min. The comparative sample with the S3 time of only 1 min without pre-etching was also measured to observe the reference peak deconvolution.

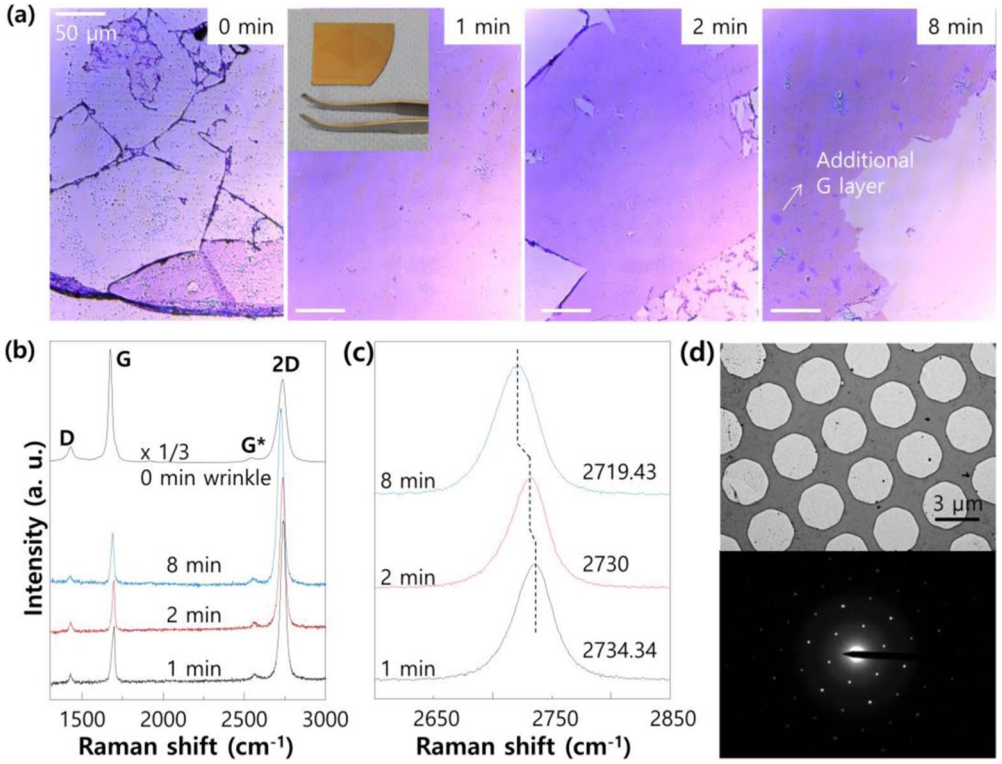

Figure 5. (a) Optical microscope image of graphene transferred on SiO_2 covered Si(100) wafer using conventional PMMA based transfer technology. (b) Raman spectra of graphene shown in Fig. 5a and (c) enlargement near the 2D band area. (d) Top: TEM images of graphene (grown on 1 min pre-etched Cu foil) transferred onto Quanti-foil TEM grid with 3 μm hole pattern. Bottom: selective area electron diffraction from graphene.

graphene and target substrate cause non-uniform adhesion during the process. From the Raman analysis shown in Fig. 5b, it is possible to obtain the structural information of the synthesized graphene. The Raman spectrum shows typical features of the monolayer graphene: (i) a 2.0 ∼ 3.0 2D/G intensity ratio and (ii) a symmetric 2D band centered with a full width at half maximum (FWHM) of ∼40.2 cm^{-1} for 1 min, ∼41 cm^{-1} for 2 min, and ∼45.4 cm^{-1} for 8 min pre-etching.[22] All samples have a weak D and G^* band and are avoidable in graphene samples grown on polycrystalline Cu foil using CVD. The red-shift of the Raman peak and increased FWHM (shown in Fig. 5c) could be due to the increased an-harmonic scattering of those optical phonons that are active in the Raman scattering processes due to the additional graphene layer as shown in Fig. 5a. As the free-standing graphene is an ideal form in which to study its unique physical properties, many trials have been carried out to make graphene large and uniform using several methods such as transfer to hole-barrier pattern and back-side Cu foil etching. In this work, we used a commercial Quanti-foil TEM Cu grid with a 3 μm hole size. We were able to cover 80% of the holes with graphene grown on pre-etched Cu foil (1 min) using the conventional transfer process. In the selected area electron pattern (SAED) images shown in Fig. 5d (the opened aperture size is about 1 μm), it was fully single crystal with single-layer (similar diffraction intensity between first order and second order). We had measured the electrical properties (mobility) of graphene. The mobility values of pre-etched Cu foil based on field effect transistor were between 2,000∼4,000 $cm^2V^{-1}sec^{-1}$. The mobility of graphene on bare Cu foil is similar with this value if there is no particle between source and drain electrode (gap is 4 μm). However, if there are nano-particles between electrodes, the mobility decreased significantly below 2,000 $cm^2V^{-1}sec^{-1}$. Although we did not measure the optical properties such as transmittance, we can expect scattering effect of light for the graphene on bare Cu foil due to residual metal-oxide nano-particles.

Conclusions

In this work, we improved the quality of graphene grown on Cu foil using the pre-reduction method (dipping of Cu foil in $(NH_4)_2S_2O_8$ solution before graphene growth on the foil). This method can be used to efficiently remove the adsorbed oxygen and water molecules which form chemical bonds such as CuO_2 and $Cu(OH)_2$ with Cu, resulting in high quality graphene. The superior quality of graphene was checked by microscopy and the chemical bonds analysis using X-ray photoemission (low sp^3 / sp^2 C-C bonds signal ratio) and Raman measurement (large 2D/G ratio and small D peak) also proved that. We believe this simple method is an ideal candidate for high quality graphene growth on a metal catalyst using the CVD system.

Acknowledgments

This work was supported by the new faculty research fund of Ajou University.

References

1. X. S. Li, W. W. Cai, J. H. An, S. Kim, J. Nah, D. X. Yang, R. Piner, A. Velamakanni, I. Jung, E. Tutuc, S. K. Banerjee, L. Colombo, and R. S. Ruoff, *Science*, **324**, 1312 (2009).
2. K. S. Novoselov, V. I. Fal'ko, L. Colombo, P. R. Gellert, M. G. Schwab, and K. Kim, *Nature*, **490**, 192 (2012).
3. A. K. Geim, *Science*, **324**, 1530 (2009).
4. K. S. Kim, Y. Zhao, H. Jang, S. Y. Lee, J. M. Kim, K. S. Kim, J.-H. Ahn, P. Kim, J.-Y. Choi, and B. H. Hong, *Nature*, **457**, 706 (2009).
5. S. Bae, H. Kim, Y. Lee, X. F. Xu, J. S. Park, Y. Zheng, J. Balakrishnan, T. Lei, H. R. Kim, Y. I. Song, Y.-J. Kim, K. S. Kim, B. Özyilmaz, J.-H. Ahn, B. H. Hong, and S. Iijima, *Nat. Nanotechnol.*, **5**, 574 (2010).
6. H. K. Yu, K. Balasubramanian, K. Kim, J.-L. Lee, M. Maiti, C. Ropers, J. Krieg, K. Kern, and A. M. Wodtke, *ACS nano*, **8**, 8636 (2014).
7. G. H. Han, F. Guenes, J. J. Bae, E. S. Kim, S. J. Chae, H.-J. Shin, J.-Y. Choi, D. Pribat, and Y. H. Lee, *Nano Lett.*, **11**, 4144 (2011).
8. H. S. Song, S. L. Li, H. Miyazaki, S. Sato, K. Hayashi, A. Yamada, N. Yokoyama, and K. Tsukagoshi, *Sci. Rep.*, **2**, 337 (2012).
9. R. M. Iost, F. N. Crespilho, L. Zuccaro, H. K. Yu, A. M. Wodtke, K. Kern, and K. Balasubramanian, *ChemElectroChem*, **1**, 2070 (2014).
10. K. L. Chavez and D. W. Hess, *J. Electrochem. Soc.*, **148**, G640 (2001).
11. I. Vlassiouk, M. Regmi, P. Fulvio, S. Dai, P. Datskos, G. Eres, and S. Smirnov, *ACS nano*, **5**, 6069 (2011).
12. X. Zhang, J. Ning, X. Li, B. Wang, L. Hao, M. Liang, M. Jin, and L. Zhi, *Nanoscale*, **5**, 8363 (2013).
13. M. P. Levendorf, C. S. Ruiz-Vargas, S. Garg, and J. Park, *Nano Lett.*, **9**, 4479 (2009).
14. Q. Hao, B. Wang, J. A. Bossard, B. Kiraly, Y. Zeng, I.-K. Chiang, L. Jensen, D. H. Werner, and T. J. Huang, *J. Phys. Chem. C*, **116**, 7249 (2012).
15. B. Zhang, W. H. Lee, R. Piner, I. Kholmanov, Y. Wu, H. Li, H. Ji, and R. S. Ruoff, *ACS Nano*, **6**, 2471 (2012).
16. Z. Luo, Y. Lu, D. W. Singer, M. E. Berck, L. A. Somers, B. R. Goldsmith, and A. T. C. Johnson, *Chem. Mater.*, **23**, 1441 (2011).
17. W.-Y. Ko, W.-H. Chen, S.-D. Tzeng, S. Gwo, and K.-J. Lin, *Chem. Mater.*, **18**, 6097 (2006).
18. K. Hong, H. K. Yu, I. Lee, K. Kim, S. Kim, and J.-L. Lee, *Adv. Mater.*, **22**, 4890 (2010).
19. C. Mattevi, H. Kim, and M. Chhowalla, *J. Mater. Chem.*, **21**, 3324 (2011).
20. I. Retzko and W. E. S. Unger, *Adv. Eng. Mater.*, **5**, 519 (2003).
21. W. S. Lim, Y. Y. Kim, H. Kim, S. Jang, N. Kwon, B. J. Park, J.-H. Ahn, I. Chung, B. H. Hong, and G. Y. Yeom, *Carbon*, **50**, 429 (2012).
22. L. M. Malard, M. A. Pimenta, G. Dresselhaus, and M. S. Dresselhaus, *Phys. Rep.*, **473**, 51 (2009).